Izv. VUZ «AND», vol.10, № 3, 2002

SPECKLE DIAGNOSTICS OF RELAXATION PROCESSES IN NON-STATIONARY SCATTERING SYSTEMS

D.A. Zimnyakov, A.P. Sviridov, A.I. Omel'chenko, V.A. Trifonov, D.N. Agafonov, P.V. Zakharov, L.V. Kuznetsova

Coherent optical method of the study of non-stationary mass transfer in scattering systems on the basis of statistical analysis of spatial-temporal fluctuations of speckle intensity is considered. Non-stationary mass transfer in the case of saturating liquid phase evaporation from a disordered porous layer and structure modification of IR-laser-mediated cartilage tissue are discussed as the possible applications of the developed speckle-diagnostical technique. For liquid phase evaporation from a porous layer, the specific feature such as the anomalous broadening of spectra of speckle intensity fluctuations with decrease of the liquid phase evaporation rate was found out. This feature is caused by peculiarities of development of the fractal-like interface between liquid and gaseous phases in a porous layer. In the case of the thermally induced structure modification of a cartilage tissue, the hysteresis-like form of dependence of the time-averaged contrast of speckle-modulated tissue image on the tissue temperature inside the treatment zone is characteristical. The effect of cartilage thermal modification is presumably caused by the «bound-to-free water» transition in the proteoglycane aggregates as one of the basic components of the tissue structure.

1. Introduction

Statistical analysis of random interference patterns, or *speckle patterns*, that appear as a result of the coherent light propagation in scattering media is the one of universally adopted techniques for probing the structural and dynamic properties of weakly ordered condensed matter. The possibility to study the dynamic behavior of ensembles of moving particles at length scales of the order of the wavelength of probe light by means of the correlation analysis of scattered light intensity fluctuations stimulated a great number of experimental and theoretical works dedicated to various aspects of the quasi-elastic light scattering by non-stationary random media. Such well-known speckle technology as the *diffusing-light spectroscopy* (DWS) [1] is now widely used for material testing in various areas of science and technology; there are many classical examples of successful applications of the DWS method and related technologies in studying such complicated processes as a Brownian dynamics of particles in suspensions, a granular flow, a foam formation, a growth of colloidal aggregates and crystallization, etc. (see e.g. Refs 2-6).

In biomedical optics, the statistical and correlation analysis of dynamic speckle patterns induced due to laser light scattering by living tissues is the physical basis for various techniques widely applied for the blood microcirculation monitoring, the burned tissue diagnostics, the cerebral blood flow visualization, etc. [7-14].

Also, the significant research activity in this field was stimulated by existence of fundamental phenomena appearing in the case of scattering of classical waves by disordered systems (such as, e.g., the long-range spatial and temporal correlations of multiply scattered field, the «memory» effect, the effect of coherent backscattering) and demonstrating certain analogies with such quantum-mechanical effect as the electron localization in disordered conductors (the so-called Anderson localization) [15-20].

The goal of this work is to review some novel techniques and results in the field of speckle diagnostics of structural and dynamic properties of weakly ordered multiple scattering media. These techniques are:

1) the study of a non-stationary mass transfer in disordered and ordered porous media on the basis of spectral analysis of dynamic speckle patterns induced by coherent light scattering in porous media;

2) the speckle contrast monitoring of structural changes in collagenous tissues induced by thermal denaturation or modification under laser heating.

On the one hand, the development of these speckle techniques gives the new opportunities in studying the complicated dynamic behavior of real systems with stochastic structure such as, e.g., the structural relaxation forced by thermal processes or non-stationary mass transfer. On the other hand, these methods are based on certain fundamental effects related to light propagation in random media at mesoscopic length scales such as the correlation transfer [21], the evolution of a polarization state of propagating light [22-25], the manifestation of the coherence phenomena in multiple-beam stochastic interference, etc. Thus, we can hope that further development of the above mentioned speckle-based methods leads us to better understanding of processes accompanying the light-matter interaction at microscopic and mesoscopic levels.

2. Speckle correlometry as applied to study the interface growth in porous media

One of the possible applications of the speckle-correlation technologies in studying a dynamic behavior of stochastic systems is the analysis of growing phenomena in porous media (e.g. in the course of the evaporation of saturating liquid phase [26] or the development of liquid-gaseous interfaces driven by capillary forces). The specific property of these growth processes is formation of the fractal-like interfaces which fractal nature is mainly caused by a structural randomness of «matrix» media. In such system, the random connections between single pores form a «stochastic network» of channels for propagation of the local boundaries between liquid and gaseous phases. The mobility of an arbitrary local boundary depends on physical properties of a liquid phase and porous medium, as well as on the characteristic size and geometry of pores. A significant variance in sizes and orientations of pores causes stochastic fractal character of the «global» interface between phases in disordered porous media. Thus, the direct observation of the time-dependent dynamics of the local boundaries that form the growing fractal-like interface is an object of great interest.

In our case, we studied such time-dependent dynamics for the case of evaporation of liquid phase from layers of wet porous media. Experimental technique was based on the spectral and correlation analysis of speckle intensity fluctuations induced by laser light scattering in layer of dried porous medium. In this case, the dynamic speckle pattern is caused by a multiple scattering of coherent light by moving local boundaries in single pores located in the vicinity of growing interface. The experimental set-up is shown in Fig. 1.

Single-mode He-Ne laser (the wavelength is 633 nm, the output power is 0.5 mW) was used as illumination source. The laser beam was focused on the surface of the wet

porous layer using a lens with the focal length of 200 mm. Scattered light was detected in the paraxial region by CCD camera (EDC-1000L, Electrim, USA) without imaging lens. The distance between the layer and CCD camera was 600 mm. Time delay and integration (TDI) mode of camera was used to get images of dynamic speckle patterns at different stages of the liquid evaporation. For this mode, the acquired image is composed as the set of 1D images of the same line in the detection plane, which are sequentially recorded with given time delay. Brightness distributions along the rows of this image correspond to temporal dynamics of the fluctuating intensity in the points of the chosen line.

Paper layers of different nature, such as copy paper and filter paper of different thickness and porosity, were used in our experiments as the layers of the disordered porous media. Before image recording, the studied samples were wetted by quickly evaporating liquid, such as ethanol or acetone. For each paper sample, the thickness and average porosity were measured. Also, such parameter as the relaxation time t_{rel} was used to characterize the studied systems «porous layer-wetting liquid». It was measured as the time lapse corresponding to e-times decay of the liquid mass in the course of evaporation from the saturated layer. For comparison with disordered porous media, the ordered porous layers with cylindrical pores were studied in our experiment. These layers are the glass plates with hexagonally packed cylindrical channels used for fabrication of

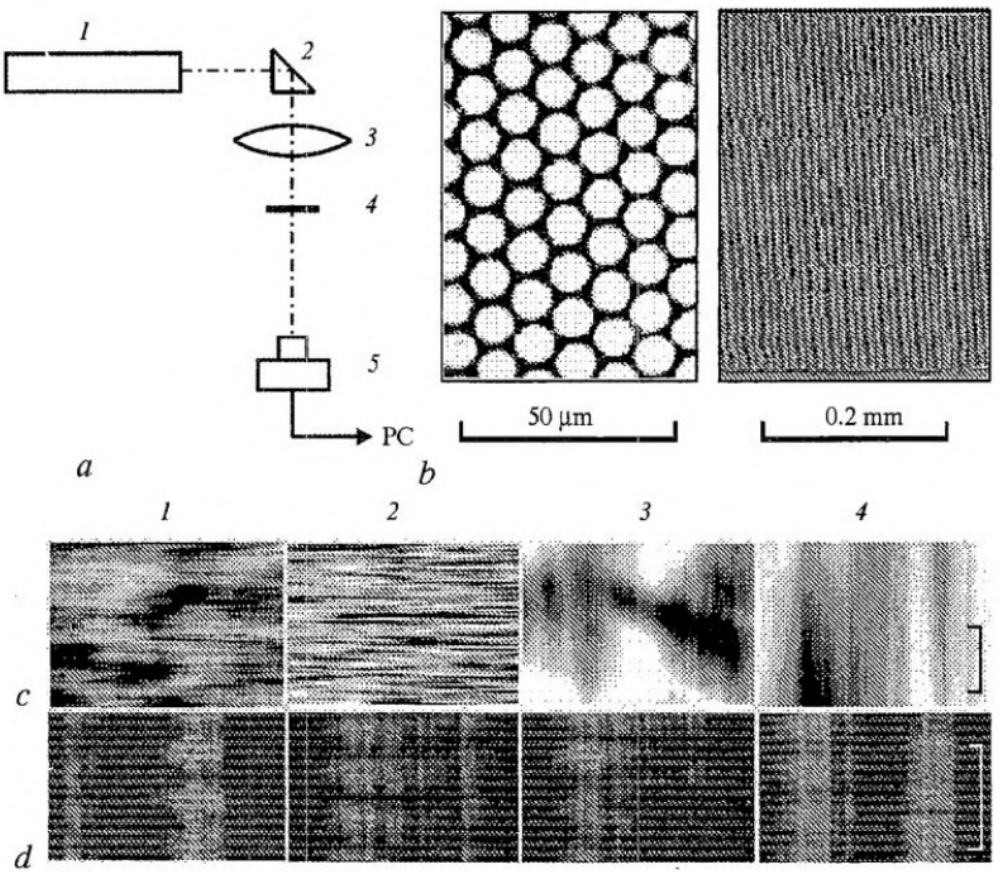

Fig. 1. *a* - scheme of the experimental setup; *1* - laser; *2* - prism; *3* - focusing lens; *4* - sample; *5* - CCD camera; *b* - photos of ordered porous sample. *c* , *d* - TDI images of dynamic speckles at different stages of wetting phase evaporation. *c* - paper layer (thickness 88 μm, porosity 0.56) wetted by acetone; *1* - t_{dr}=10 s; *2* - t_{dr}=35 s; *3* - t_{dr}=240 s; *4* - t_{dr}=320 s; bar - 10 s. *d* - sample as in Fig. 1*b*, wetted by ethanol; *1* - t_{dr}=30 s; *2* - t_{dr}=100 s; *3* - t_{dr}=400 s; *4* - t_{dr}=580 s; bar - 10 s

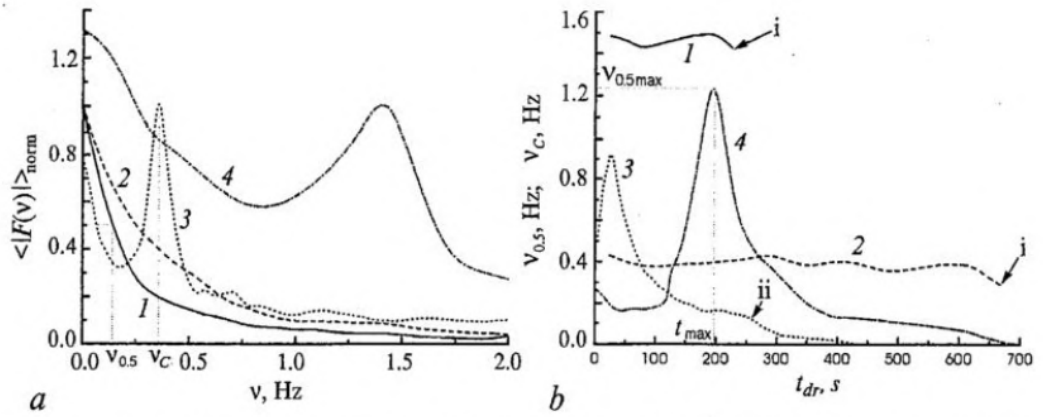

Fig. 2. *a* - typical forms of the normalized Fourier spectrum module of intensity fluctuations for paper layer (thickness 71 μm, porosity 0.68, ethanol) (*1*, *2*) and for ordered sample (Fig. 1,*b*) (*3*, *4*) wetted by ethanol (*3*) and acetone (*4*). *1* - t_{dr}=23 s; *2* - t_{dr}=150 s; *b* - the dependencies of ν_c (*1*, *2*; sample as in Fig. 1, *b*) and $\nu_{0.5}$ (*3*, *4*; paper sample, thickness 88 μm, porosity 0.56) on t_{dr}. Wetting liquid - acetone (*1*, *3*) and ethanol (*2*, *4*); i - final stage of evaporation; ii - presumable stage of clusterization

the micro-channel plates (MCP) (Fig. 1, *b*). The fragments of typical speckle images for different stages of the liquid evaporation are shown in Fig. 1, *c*, *d*.

For each frame of a sequence of acquired TDI images, the averaged module of the Fourier spectrum of speckle intensity fluctuations was calculated for pixel brightness distributions along each row, using the averaging of values of the spectrum module over the set of rows. The typical forms of the normalized spectrum module are shown in Fig. 2 for disordered and ordered porous media. In the first case, motions of the local boundaries in the porous layer cause the speckle intensity fluctuations in the form of band-limited random process with spectrum half-width $\nu_{0.5}$ depending on the average boundary mobility.

For ordered porous layer, the observed speckle dynamics has quasi-periodic character (Fig. 1, *c*) with center frequency ν_C depending on the average velocity of local boundaries propagation.

The typical dependencies of $\nu_{0.5}$ for disordered layer and ν_C for ordered layer on evaporation time t_{dr} are shown in Fig. 2, *b*.

Non-monotonic behavior of $\nu_{0.5}$ with increase of t_{dr} and appearance of its maximum value at certain stage of evaporation characterized by t_{max}, can be mentioned as specific property of the observed speckle dynamics in case of disordered layers. It was found for all studied paper samples, that t_{max} and t_{rel} are related as $t_{max} \sim t_{rel}^{1.08\pm0.10}$. Another feature is that despite the higher mobility of the local boundaries in the case of acetone as evaporating liquid, the speckle dynamics for disordered porous structure is characterized by less values of $\nu_{0.5max}$ than for ethanol (for comparison, see dependencies of ν_C on t_{dr} for ordered porous layer).

These peculiarities can be interpreted in terms of multiple light scattering by a non-stationary ensemble of local boundaries in disordered porous layer. Non-monotonically changing $\nu_{0.5}$ with the increasing time lapse t_{dr} of liquid evaporation is caused by variation of concentration of dynamic scatters (i.e. local boundaries) in the scattering volume. This is due to the effect of multiplication of a random Doppler shift for each scattering event by an effective number of scattering events. This number

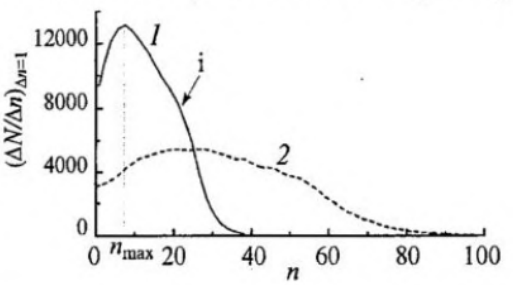

Fig. 3. The dependence of node release rate on *n*. N_1=N_2=100; N_3=30; Ω=6. *1* - *P*=0.3; *2* - *P*=0.1; i - stage of clusterization

for multiply scattering system depends on the parameter $(L/l^*)^2$, where L is the characteristic size of the scattering system and l^* is the effective value of the transport mean free path depending on the scatter concentration [1,19,27]. For drying disordered porous layer, the growth of fractal interface [28] between phases causes simultaneous changes in L (which is related to the interface «height») and in l^* (which is proportional to the inverse of concentration of moving local boundaries in the zone of interface growth). In the case of a slab scattering geometry, the decay of temporal correlation of fluctuating scattered field depends on the dimensionless parameter $k^2\langle\Delta\bar{r}^{\,2}(\tau)\rangle(L/l^*)^2$ [19,27], where k is the wave-number of light in the scattering medium, $\langle\Delta\bar{r}^{\,2}(\tau)\rangle$ is the variance of the scatter displacements for the time lapse τ and L is the slab thickness. The value of $\langle\Delta\bar{r}^{\,2}(\tau)\rangle$ can be considered as corresponding to the generalized Brownian motion of the scattering sites: $\langle\Delta\bar{r}^{\,2}(\tau)\rangle=K\tau^{\vartheta}$, where K is determined by scatter mobility and ϑ depends on dynamic properties of the scattering system.

The rigorous analytical form of the temporal correlation function of field fluctuations is determined by scattering conditions and optical properties of the scattering medium, such as the diffuse reflectivity and can be found only for a limited number of the diffuse-scattering systems [27]. However, from the principle of similarity it follows that the correlation time τ_c of field fluctuations varies as $\tau_c\sim(l^{*2}/k^2KL^2)^{1/\vartheta}$ in the dependence on the parameters of scattering system. Considering the porous layer initially wetted by liquids with approximately equal values of refractive index and assuming the same dynamical properties of the ensemble of local boundaries ($\vartheta_1=\vartheta_2=\vartheta$) but different mobility parameters ($K_1\neq K_2$), the ratio of $\nu_{0.5max}$ can be expressed as:

$$(\nu_{0.5max})_1/(\nu_{0.5max})_2 = (\tau_{max})_2/(\tau_{max})_1 = \\ = \{K_{1max}L_{1max}{}^2 l_{2max}{}^{*2}/K_{2max}L_{2max}{}^2 l_{1max}{}^{*2}\}^{1/\vartheta}. \quad (1)$$

The ratio $l_2^*/_1^*$ can be modified using the relation for the transport mean free path: $l^*=\{c\sigma(1-g)\}^{-1}$, where c, σ and g are the effective values of the concentration, scattering cross-section and anisotropy parameter of moving scattering sites (local boundaries). We can assume that for wetting liquids with close values of the refractive index ($n_1\approx1.354$ at 633 nm for acetone and $n_2\approx1.358$ for ethanol) the effective values of σ and g are approximately equal and the ratio $l_2^*/_1^*$ can therefore be reduced to c_1/c_2.

Hence, we obtain:

$$(\nu_{0.5max})_1/(\nu_{0.5max})_2 = \{K_{1max}\gamma_{1max}{}^2/K_{2max}\gamma_{2max}{}^2\}^{1/\vartheta}, \quad (2)$$

where the parameter $\gamma=\tilde{L}c$ characterizes the effective surface density of dynamic scattering sites, or the number of stochastically moving local boundaries per unit area of porous layer.

Computer simulation of stochastic irreversible growth of interfaces in 3D lattices with different number of connections Ω between nodes was used to analyze the behavior of the ratio γ_1/γ_2 in the course of interface growth. The simulation model was similar to the Eden model [29]. At the initial moment, the $N_1\times N_2\times N_3$ lattice ($N_1=N_2>>N_3$) was assumed consisting of occupied nodes. Interface growth is related to sequential release of the occupied nodes beginning from the lattice boundaries. Each occupied node can be released with given probability P at the current simulation step if it has at least one connection with free neighboring nodes released at previous steps. The number of connections Ω per lattice cell as the model parameter was varied from 6 (the simple cubic lattice) to 14 (the cubic lattice with «diagonal» connections between layers). The growth process for each set of simulation parameters was characterized by the relaxation parameter n_{rel} evaluated as the number of steps corresponding to e-times decay of the amount of occupied nodes.

The extreme case of P=1 leads to appearance of the «conventional» non-fractal interface propagating in the lattice with constant velocity. Decreasing probability of the node release causes the fractal-like growing interfaces with the increasing height of the growth zone for a given position of interface. Despite the simplicity of this model, it has allowed us to interpret the general features of the interface growth in porous layers that are manifested in the observed spectra of scattered light fluctuations. Typical behavior of the amount of nodes $(\Delta N_f/\Delta n)_{\Delta n=1}$ released at each step is illustrated by Fig. 3 as depending on the number of steps.

The maximal value $(\Delta N_f/\Delta n)_{\Delta n=1}$ obtained at $n=n_{max}$ corresponds to maximally developed interface between the regions of occupied and free nodes. Analysis of the relation between n_{max} and n_{rel} leads to the approximately linear dependence $n_{max}\sim G n_{rel}^{1.05\pm0.10}$ for $0.001\le P\le 0.5$ and $6\le\Omega\le 14$, where G depends on the model parameters P, Ω, $N_1=N_2$, N_3. Such tendency is very similar to the above mentioned relation between the measured values of t_{max} and t_{rel}. Evaluations of effective surface density of occupied nodes for the zone of growth made at $n=n_{max}$, show it as monotonically decaying to the value close to 1 with increasing P (Fig. 4). In contrast, values of γ_{max} estimated for small values of P, are close to 3 as a manifestation of the growing interface fractality. In the case of relatively high growth rates ($P\ge$0.20-0.25), the dependencies of $(\Delta N_f/\Delta n)_{\Delta n=1}$ on n show the appearance of the sharp decay in this parameter at final stage of release of nodes, which corresponds to the division of the region of occupied nodes into separate clusters at the final stage of growth (Fig. 3, marked by arrow). This peculiarity appears «smoothed» at low growth rates. Similar tendencies can be mentioned for experimentally obtained curves $\nu_{0.5}(t_{dr})$ (Fig. 2, *b*), where the noticeable sharp decay in $\nu_{0.5}$ takes place at the final stage of acetone evaporation (marked by arrow). In contrast, similar curve for ethanol is characterized by the significantly less peculiarity of this type.

The ratio of K_1/K_2 was estimated using a consideration of the mass transfer of evaporating phase for the zone of interface growth. The following relation can be written for the mass flux from the growth zone: $|J|\approx C\rho\langle a\rangle^2 c\tilde{L}\langle S\rangle_{\tau=1}$, where C is the dimensionless parameter related to the pore geometry, ρ is the liquid density, $\langle a\rangle$ is the characteristic size of the pore cross-section and $\langle S\rangle_{\tau=1}$ is the average path travelled by moving local boundaries per unit time. With used assumptions, the traces of moving local boundaries can be considered as the fragments of 3D fractal curves characterized by the fractal dimension equal to $2/\vartheta$ [30]. Estimation of the average length of trace $\langle S\rangle_{\tau=1}$ by use of the average boundary displacement per unit time $\langle\Delta\bar{r}^{\,2}(\tau=1)\rangle^{1/2}=K^{1/2}$ as the scale gives the following relation: $\langle S\rangle_{\tau=1}\sim K^{1/\vartheta}$ and, correspondingly, $|J|\sim K^{1/\vartheta}\gamma$. Thus, for the same

Table

The estimated values of ϑ; subscript «1» corresponds to acetone as wetting liquid; «2» - to ethanol

Sample	t_{max1}, s	t_{max2}, s	$(\nu_{0.5max})_1$, Hz	$(\nu_{0.5max})_2$, Hz	ϑ
1[a]	≈46	≈286	≈0.59	≈0.65	≈1.05
2[b]	≈31	≈195	≈0.92	≈1.21	≈0.96
3[c]	≈54	≈207	≈0.78	≈1.42	≈1.04

[a] Filter paper; thickness 135 μm, porosity 0.84;
[b] Copy paper; thickness 88 μm, porosity 0.56;
[c] Copy paper; low quality; thickness 71 μm, porosity 0.68.

porous system saturated by liquids with $\rho_1 \approx \rho_2$ and different values of K, the ratio K_1/K_2 can be expressed as $\{(J_1/\gamma_1)/(J_2/\gamma_2)\}^{\vartheta}$. The parameter J/γ at $t_{dr}=t_{max}$ is related to the value of t_{max}. For the simulation model, the following relation between $(\Delta\tilde{N}_f/\Delta n)_{max}/\gamma_{max}$ and n_{max} was obtained for $0.001 \le P \le 0.5$: $(\Delta\tilde{N}_f/\Delta n)_{max}/\gamma_{max} \sim n_{max}^{-\beta}$, where the value $(\Delta\tilde{N}_f/\Delta n)_{max}/\gamma_{max}$ was estimated for unit area of the zone of growth and β is of the order of 1 ($\beta=1.00\pm0.05$). Assuming the similar relation between J_{max}/γ_{max} and t_{max} for studied porous samples, we obtain the approximating relation:

$$(\nu_{0.5max})_1/(\nu_{0.5max})_2 = (t_{max2}/t_{max1})\{\gamma_{max1}^2/\gamma_{max2}^2\}^{1/\vartheta}. \quad (3)$$

For paper layers saturated by acetone and ethanol, the measured ratios t_{max2}/t_{max1} vary from 4 to 6.5, depending on paper porosity and density. The ratios $(\nu_{0.5max})_1/(\nu_{0.5max})_2$ vary between 0.4 and 1.0. The measured typical values of these parameters for three paper samples are presented in the Table. The results of simulation of irreversible growth (Fig. 4) allow us to estimate $\gamma_{max1}/\gamma_{max2}$ for two porous systems with $K_1 >> K_2$ as the values of the order of 2.5 - 3.0; this leads to the value of ϑ close to 1 (estimations of ϑ made for the value of $\gamma_{max1}/\gamma_{max2}$ equal to 2.75, are presented in the Table).

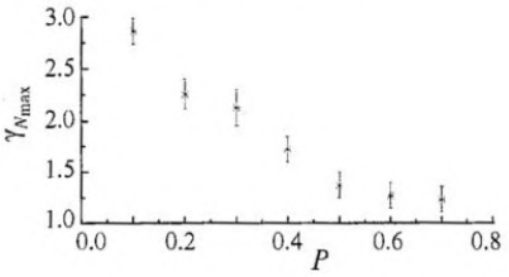

Fig. 4. The effective surface density of released nodes vs node release probability at $n=n_{max}$ (results of simulation); $N_1=N_2=100$; $N_3=30$; $\Omega=6$

Hence, the typical magnitudes of ϑ obtained from experimental results allow us to suppose that the dynamics of local boundaries, which causes the interface growth in the course of liquid phase evaporation from stochastic porous layers such as paper, is in general similar to the «classical» Brownian dynamics.

3. Speckle-contrast-based monitoring of the tissue structure modification

Analysis of spatial-temporal fluctuations of scattered coherent light is a modern approach in the study of non-stationary scattered systems, such as living tissues. We can enumerate many examples of applying quasi-elastic scattering methods for tissue diagnostics. These involve above mentioned modifications of laser Doppler flowmetry (see, e.g., Refs [7, 8]) and DWS technique as applied to blood microcirculation monitoring and burned tissue diagnostics [9], laser speckle contrast analysis (LASCA) for similar applications [10-12, 14], and speckle contrast measurements in study of mechanical properties of tissues [13].

One of possible approaches in the study of spatially heterogeneous non-stationary media by the use of the speckle technologies is the contrast analysis of time-averaged dynamic speckle patterns in the image plane. In this case the image of object surface, which is illuminated by coherent light, is recorded with the exposure time T comparable with the correlation time τ_c of intensity fluctuations of image-modulating dynamic speckles. This causes the blurred speckle pattern on the recorded image, which is characterized by the reduced value of contrast decaying with increase of T/τ_c ratio. For tissue images captured with T=const, the presence of dynamic macro-inhomogeneities in the scattering volume (such as, e.g., large vessels or local variations of the blood perfusion level) will induce the spatial variations of the locally estimated contrast for blurred image-modulating speckles. This effect can be applied to functional imaging of living tissues by the use of local estimates of the speckle contrast as the visualization

parameter; in particular, such imaging technique was discussed in Refs [10, 11]. More recent example of speckle imaging of living tissues is application of the LASCA technique for visualization of cerebral blood flow reported in Ref. 14.

Here we present the results of the contrast analysis of time-averaged dynamic speckle patterns to monitor the structure modification of thermally treated collagenous tissue, such as cartilage. Laser-induced thermal reshaping of cartilage is a modern approach in laser medicine [31]. One of the probable mechanisms of this reshaping is presumably related to «bounded-to-free» water transition induced in macro-molecular structure of proteoglycan aggregates (PGA), one of the components of cartilage tissue [32, 33]. Another thermally activated mechanism of tissue reshaping is the partial thermal denaturation of the collagen matrix as the second basic component of cartilage tissue. In particular, the changes in mechanical properties of thermally treated collagen were studied in Ref. [34], where the empirical relations between mechanical properties of the thermally modified tissue, its shrinkage as a result of thermal modification, treatment temperature and time duration of a treatment procedure were established. It was found that mechanical properties decreased with increasing shrinkage, and that the maximal allowable shrinkage before significant material property changes occurred was between 15% to 20%. At larger values of tissue shrinkage, the progressive increase of the proportion of collagen fibrils undergoing denaturation was observed by means of the transmission electron microscopy. The abrupt increase in the tissue shrinkage rate was observed at the temperatures above 60 ° C.

Recent studies also revealed the existence of noticeable changes in physical and mechanical characteristics of the heated cartilage in the narrow temperature region near 70° C [31-33]. In particular, changes in tissue scattering properties were observed for this temperature range in the course of thermal treatment of cartilage. This effect was interpreted in terms of water release from heated zone and subsequent decrease of scattering centers sizes [35].

Also, the alterations of mechanical properties of the cartilage during the tissue treatment that are, for instance, revealed as the relaxation of the internal stress, are related to the time-dependent inhomogeneous deformation of tissue. In its turn, the process of thermal treatment of cartilage tissue illuminated by coherent light must be accompanied by expressed speckle dynamics of scattered optical field due to the time-dependent mutual local displacements of scattering sites such as collagen fibrils that form the tissue matrix. This is why statistical analysis of speckle intensity fluctuations can be used for monitoring of modification processes. The importance of such monitoring for laser reshaping of the native cartilage is caused by the necessity to provide conditions for proper tissue modification and to avoid the dramatic changes in cartilage structure caused by collagen denaturation in the treatment zone.

In experiments, the transmittance mode of probe He-Ne laser light propagation through a layer of thermally modified cartilage tissue was chosen to study the temperature-dependent dynamics of image-modulating speckles. Fig. 5, *a* shows the scheme of experimental setup. Single-mode He-Ne laser (1) (633 nm, linear polarization, output power 5 mW) was used as a light source. Laser beam was expanded by 50$^{\times}$ telescopic system (2) and put on the front surface of ex-vivo sample (3) of porcine cartilage. Samples were prepared as 15 mm×25 mm pieces of 1.5 mm thickness. Speckle-modulated images of the sample back surface were captured by CCD-camera (5) (EDC-1000L, Electrim, USA) with zoom lens (4) (LMZ13A5M, 12.5-75 mm). Such detection geometry causes relatively high level of the detected light intensity and relatively low-frequency intensity fluctuations for image-modulating speckles, or their slow dynamics, in comparison with detection of the backward scattered light due to typically small values of the scattering angle. This had allowed us to choose the appropriate parameters of the image acquisition procedure for the range of exposure times and frame recording rates

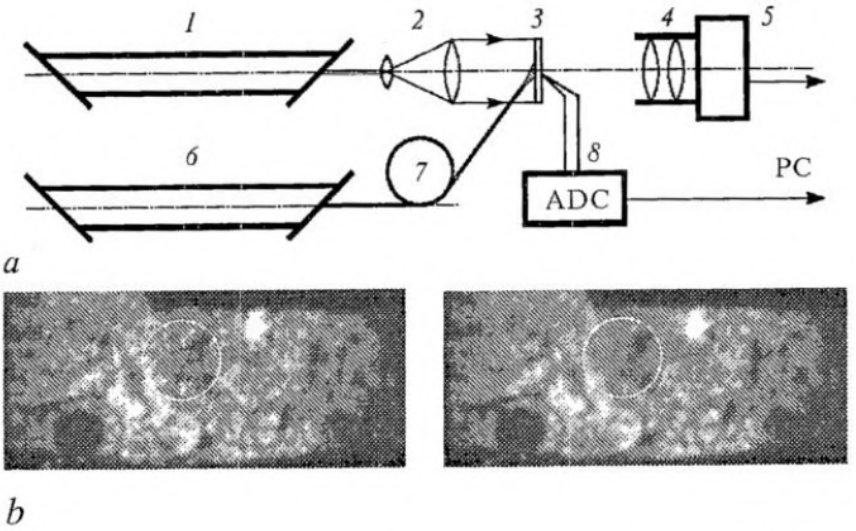

Fig. 5. *a* - scheme of the experimental setup; *b* - time-averaged images of the treated tissue; left panel - before treatment; right panel - during the treatment; treatment zone is marked by white circle

typical for used video capture system and, in its turn, to provide the detailed analysis of slow speckle dynamics for the treatment zone. Besides, image analysis with use of the transmitted light allows us to exclude an influence of the tissue surface reflection on speckle pattern formation that in this case is caused only by the bulk scattering into the probed volume.

Optimal conditions for speckle-modulated image recording are determined by two concurring factors that depend on the aperture of imaging lens: the appropriate mean size of speckles in the image plane and the appropriate brightness of speckle-modulated image captured with exposure time that is comparable with the correlation time of speckle intensity fluctuations. The larger average size of image-modulating speckles in the case of smaller imaging lens aperture leads to minimization of distortions of speckle statistics caused by the finite photosensitive area of each CCD pixel. But the decrease of imaging lens aperture causes a decrease of average brightness of image captured with given exposure time and, as a result, a decrease in the dynamic range of detected speckle intensity and the signal-to-noise ratio. For used experimental conditions and typical values of the correlation time of speckle intensity fluctuations, the optimal value of imaging lens aperture was found to be of the order of $f/12$, where f is the focal length of the imaging lens. In this case, the estimated average speckle size in the image plane was 10 - 12 μm; this value is comparable with the pixel size for used CCD camera and thus the integration of spatial intensity fluctuations over each local detection zone (CCD pixel photosensitive area) takes place. On the basis of the sampling theorem (see, e.g., Ref. [36]), these detection conditions will cause the certain diminishing of the estimated contrast values due to the low-frequency spatial filtering properties of the detector in comparison with the ideal detection conditions, when the speckle size is much larger than the CCD pixel size, and a great number of image-modulating speckles is covered by the whole CCD photosensitive area.

Thermal treatment of the sample was provided by Erbium fiber laser (6) (λ=1.56 μm, output power up to 3.5W) with multimode quartz fiber (7) (0.6 mm diameter) as a light-delivering system (LS-1,5, IRE-Polus, Russia). The wavelength of 1.56 μm provides the bulk absorption of laser radiation by tissue and corresponds to the edge of one of the water absorption bands in the near infrared region [36]. For tissue, the penetration depth of treating laser radiation is of the order of 1 mm. The fiber tip was placed at 15 mm from the sample surface and the diameter of treatment zone was about 4

mm. Thin wire thermocouple (30 μm in diameter, (8)) was used to control the current tissue temperature T in the central part of the zone. It was embedded into the sample so that the distance from the nonirradiated back surface of the sample was about 0.5 mm. The use of such thin thermocouple provides locality and fast response of dynamic measurements of the sample temperature. Notice that direct laser heating of thermocouple tip may cause some error. Our rough theoretical estimates of a maximal difference between the temperature of the laser-heated thermocouple and that of surrounding medium were made using the comparison of the heat transfer from thermocouple body to medium and heat deposition due to laser irradiation. These estimates give the difference about 3° C for typical values of the used beam intensity. In practice, this difference should be much less due to simultaneous heating by laser as thermocouple and tissue. Indeed, at high absorption coefficient of tissue the temperature of thermocouple may be less than the tissue temperature despite its being heated by laser. As to our experiments, the validity of the thermocouple use is obliquely confirmed from cooling dynamics measured immediately after the laser was switched off. In the case of a noticeable difference between temperatures of the thermocouple body and surrounding medium, this should cause the noticeable jump-like changes in measured temperature values because of the fast equalization of the body temperature and that of surrounding medium. Any distortions of this form at the initial stage of sample cooling were not observed in our case. Notice finally that the tissue subsurface temperature near the back surface should be slightly less than the temperature near the irradiated surface.

Sequential recording of speckle-modulated images of sample surface was carried during the laser treatment and after the laser was switched off. After the capture of frame sequences, the time series averaging of speckle intensity fluctuations was carried out for each pixel in the image plane using a sampling window of given width $2K+1$:

$$\tilde{I}_{i,j}^{\,k} = \Sigma_{m=-K}^{K} I_{i,j}^{\,k+m} / (2K+1), \qquad (4)$$

where k is the number of image in the frame sequence, and i, j are the pixel coordinates in the image plane. The window width determined by the number of averaged frames was chosen in correspondence to the correlation time of intensity fluctuations in the center of treatment zone. The number of averaged frames corresponding to the window width varied from 3 to 7 for typical image capture parameters (exposure is 10 ms, sampling interval Δt is 400 ms). This scheme of speckle-modulated image processing is based on the fundamental relations between statistical properties of the spatial-temporal fluctuations of dynamic speckles. Such relations allow the evaluation of the correlation time of speckle intensity fluctuations by the use of analysis of exposure-dependent speckle contrast as applied to time-averaged images of dynamic speckle patterns. Our scheme of speckle-modulated image processing reproduces in general the basic steps typical for laser speckle contrast analysis (LASCA), namely:

1) recording of time-averaged dynamic speckle pattern with given exposure time (in our case this procedure is similar to construction of image by averaging over the number of sequential frames sampled by the window of given width; the advantage of this approach is related to possibility to obtain values of the time-averaged speckle intensity with high temporal resolution determined by the frame sampling interval used for the frame sequence recording; on the contrary, in the case of using traditional LASCA technique the temporal resolution is determined by the used exposure time comparable with the window width for our case);

2) statistical analysis of spatial fluctuations of the time-averaged speckle intensity; digital image processing procedure in our case is the same as for LASCA technique.

The example of time-averaged image of tissue before and during the treatment is presented in Fig. 5, *b*. Treatment zone with expressed speckle dynamics is characterized by smaller level of pixel brightness fluctuations. Averaged images were processed to

obtain the local estimates of the contrast $V_{i,j}^{\ k} = \sigma_{Ii,j}^{\ k}/\langle \tilde{I} \rangle_{i,j}^{\ k}$ for different regions of each frame obtained with the window width of $2K+1$. The time-dependent mean square root value $\sigma_{Ii,j}^{\ k}$ and the mean value $\langle \tilde{I} \rangle_{i,j}^{\ k}$ of 8-bit pixel brightness were calculated for a set of pixels inside the circular sampling area:

$$\langle \tilde{I} \rangle_{i,j}^{\ k} = (1/M)\Sigma_{m,n} \tilde{I}_{i+m,j+n}^{\ k} \Big|_{m^2+n^2 \le r^2},$$
$$\sigma_{Ii,j}^{\ k} = [(1/M)\Sigma_{m,n} (\tilde{I}_{i+m,j+n}^{\ k} - \langle \tilde{I} \rangle_{i,j}^{\ k})^2 \Big|_{m^2+n^2 \le r^2}]^{1/2}, \quad (5)$$

where r is the radius of sampling area and M is the number of pixels inside the area. The area radius was chosen at least 3 times wider than the average speckle size, but less than the treatment zone radius.

To characterize the relative changes in $V_{i,j}^{\ k}$ in the course of «thermal treatment-thermal relaxation» cycle, the normalized contrast value $\tilde{V}_{i,j}(t)=V_{i,j}(t)/V_{i,j}(0)$ was used, where $t=k\Delta t$ is the time lapse and $V_{i,j}(0)$ is the initial contrast. This normalization procedure allows us to compare the behavior of the time-averaged contrast for various treatment conditions independently on the initial contrast value that significantly varies across the imaged tissue surface. Typical behavior of $\tilde{V}_{i,j}(t)$ for central part of treatment zone is shown in Fig. 6; the dependence of current temperature T measured with use of the termocouple in the vicinity of the back surface on the time lapse is also presented. At the first stage of treatment (time lapse interval from 0 to ≈20 s), the increase of T is accompanied by the decay in $\tilde{V}_{i,j}(t)$. The second stage ($20s \le t \le 60s$) corresponds to thermally induced modification of cartilage and, being examined by the statistical properties of image-modulating speckles, is characterized by suppression of speckle dynamics that results in the increase of $\tilde{V}_{i,j}(t)$. The increasing heat loss rate at temperatures above 60° C becomes comparable with the rate of the heat deposition due to tissue irradiation by IR laser light for used treatment conditions and so causes a significant fall of the tissue temperature rate; as a result, a plateau-like region appears on the $T(t)$ dependence. The final stage, or thermal relaxation of the treated tissue, is accompanied by non-monotonic changes of the normalized contrast value with common tendency to increase.

This behavior leads to a specific, «loop-like» form of dependencies of $\tilde{V}_{i,j}(t)$ on T (Fig. 7) in the treated zone related to the irreversible thermal modification of tissue structure due to partial relieving of heterogeneously stressed collagen matrix. Thus, the evolution of dynamic scattering system such as modified cartilage tissue depending on treatment conditions can be described by a set of similar trajectories in $(T,\tilde{V})$ plane. For arbitrary trajectory the following typical stages of system evolution can be singled out and a corresponding scenario of system behavior can be considered:

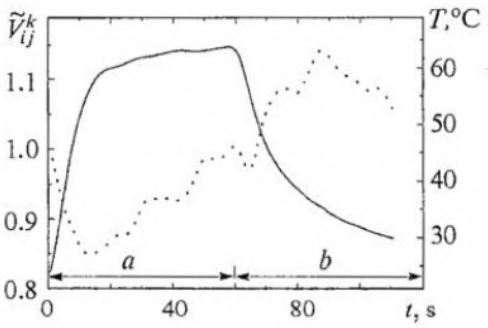

Fig. 6. The dependencies of $\tilde{V}_{i,j}(t)$ (dotted curve) and T (full curve) on t during and after the laser treatment (a and b, respectively). Er laser output P is 1.2 W

1) the stage of $\tilde{V}$ decay caused by increasing thermal deformations of heterogeneously stressed scattering structure consisting of 3D network of collagen fibres (collagen matrix) fixed by macro-mole-

cular ensemble of water-coated proteoglycane aggregates;

2) the stage of partial stress relaxation, characterized by the rapid increase in $\tilde{V}$ with slightly increasing tissue temperature; the width of loop, $\Delta\tilde{V}$, depends on the duration of the plateau-like region of $T(t)$ dependence;

3) the stage of formation of a new, partially relieved stable spatial configuration of the scattering system accompanied by decrease in $\tilde{V}$;

4) the final stage of thermal relaxation of modified cartilage structure. The behavior of the scattering system at this stage is generally similar to that described for the first stage (in particular, both fragments of $\tilde{V}(T)$ are characterized by close values of the trend line slope).

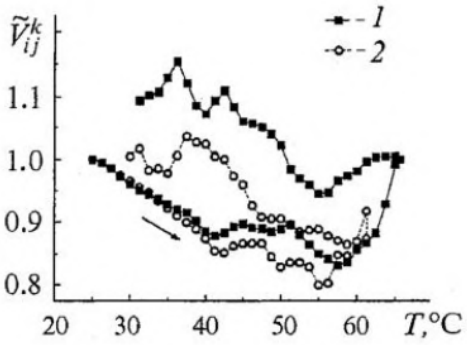

Fig. 7. The dependencies of $\tilde{V}_{i,j}(t)$ on T for treatment-relaxation cycle. Squares (1), P=1.2 W, near the center of treatment zone; circles (2), P=0.8 W, near the center of zone. Black arrow indicates the heating stage; gray arrows indicate the thermal relaxation stage

Following from experimentally observed non-monotonic behavior of the time-averaged speckle contrast with increase of the tissue temperature, we can conclude that the specific feature of cartilage thermal modification is the appearance of the additional factor changing sufficiently the thermally activated dynamic behavior of tissue scattering structure for measured values of tissue temperature above 60° C. These changes are manifested not only in variations of the speckle contrast, but also in behavior of the tissue diffuse transmittance as well as the internal stress [37]. At the initial stage of thermal treatment, the decay in $\tilde{V}$ with increasing temperature can be interpreted in terms of thermally activated irreversible local deformations of tissue collagen matrix revealed at macroscopic level as the tissue shrinkage [34]. Another well-known manifestation of thermal modification of the collagen structure due to partial denaturation are the temperature-induced changes in tissue optical properties, say, the birefringence [38]. On the basis of empirical relation between the relative value of tissue shrinkage, the temperature and the duration of thermal treatment given in Ref. 34, the instantaneous rate of thermally induced irreversible deformation of collagen fibrils can be approximately estimated as:

$$\dot{\varepsilon}(t,T) \approx - K_1(T) t^{K_2(T)-1} / (1+K_3(T) t^{K_2(T)})^2, \qquad (6)$$

where $K_1(T)$, $K_2(T)$, $K_3(T)$ are the empirically evaluated temperature-dependent coefficients. This expression gives the abrupt increase of the deformation rate with increasing temperature and its slow decay at the final stage of collagen thermal modification, when the tissue deformation exceeds 25% and collagen native structure is almost totally denaturated [34]. Mutual displacements of the structure-forming elements such as collagen fibrils in the course of tissue deformation will induce intensity fluctuations of coherent light scattered by the modified tissue structure. These intensity fluctuations are characterized by the correlation time depending on characteristic time interval required for displacement of scattering sites such as collagen fibrils at the distance of the order of the wavelength λ_0 of illuminating light and, correspondingly, are related to the scattering structure deformation rate:

$$\tau_c \sim \Lambda\lambda_0 / l\, \dot{\varepsilon} n, \qquad (7)$$

where l is the characteristic distance between scattering sites for a probed medium, n is the medium refractive index and the factor Λ depends on the average number of scattering

events, illumination and detection conditions. With the use of such simple phenomenological model, it is possible to give qualitative interpretation of the decay in the correlation time of speckle intensity fluctuations and, correspondingly, in the time-averaged speckle contrast with increasing tissue temperature that is observed at the ini tial stage of the cartilage thermal treatment. In turn, the increase of $\tilde{V}$ observed at the second stage of modification process, cannot be completely interpreted in terms of further progress in thermal modification of collagen matrix due to partial denaturation of the collagenous component of cartilage tissue. With the tissue shrinkage progress, the appearance and accumulation of new scattering centers due to thermal denaturation of collagen fibrils is rather accompanied by further decrease in correlation time of speckle intensity fluctuations or tissue transmittance. In particular, the additional study of dynamic light scattering by soft collagenous tissue such as porcine sclera in the course of its thermal denaturation at fixed temperatures in the range from 60° C to 90° C showed the monotonic decrease in the correlation time of scattered light intensity fluctuations with the increasing tissue temperature. Also, the additional oblique argument against the mechanism of the time-averaged speckle contrast increase for the temperatures slightly above 60° C that can be directly related to thermally activated denaturation of the collagen matrix, is that the thermally induced dramatic changes in collagen structure should appear for sufficiently larger values of laser beam intensity and exposure time than that used for laser-mediated cartilage reshaping. Typically, the thermally induced deformations of cartilage tissue accumulated to the final phase of the initial stage of thermal treatment, are significantly less than critical values of 15-20% given in Ref. 34. Thus, in our case we should not expect the decay in the tissue deformation rate and, correspondingly, increase of the time-averaged speckle contrast due to degradation of the collagen matrix. In particular, the examination of the cartilage after the laser treatment with an optical microscope [39,40] did not show any evidence of dramatic changes in matrix structure for appropriately chosen reshaping conditions.

Thus, the change in behavior of $\tilde{V}$ in the narrow interval of the measured tissue temperature slightly above 60 °C can be presumably related with the manifestation of one or several adequately effective thermally activated mechanisms of relaxation of the matrix deformation rate. At present time, the total physical picture of this effect is not yet fully understood but the mechanism of bounded to free water transition in the proteoglycan aggregates (PGA) structure due to dissociation of PGA macromolecules was discussed as the probable candidate for the role of such stress relaxation controlling mechanism [33]. The argument supporting this hypothesis is that the mechanical properties of cartilage tissue are strongly influenced by the interactions between subsystems of collagen matrix and PGA as the tissue basic components. Therefore, the alterations in hydrodynamic properties of PGA ensemble as the ground substance will cause the change in deformability of a whole tissue. In particular, it was found by means of a dynamic light scattering [41] that the thermal dissociation of proteoglycan macromolecules at temperatures above 60° C is accompanied by the significant increase in the translational diffusion coefficient of PGA.

In further study of tissue modification process, analysis of «loop-like» curves plotted in $(T,\tilde{V})$ coordinates (in particular, the relation between loop height $\Delta\tilde{V}$ and duration of plateau-like region on $T(t)$ curve) can be applied for evaluation of kinetic parameters of the internal stress relaxation, in addition to recently described approaches, such as the study of thermal and mechanical effects, tissue diffuse transmittance and/or reflectance measurements, FTIR spectroscopy, and examination by the use of optical and atomic force microscopy.

4. Conclusion

Presented results illustrate the potentialities of various modifications of the speckle correlometric techniques in studying the dynamic properties of local scatters that form weakly ordered multiple scattering systems of various nature. Further development of speckle-based coherent optical technologies can be related to the application of polarization discrimination of multiple scattered speckle patterns as well as the use of partially coherent probe light with the controllable coherence length. These approaches open the way for precise analysis of the light transfer processes in disordered scattering systems due to possibility of selection of partial components of multiple scattered optical fields with given pathlength distributions.

This work was supported in part by CRDF grant REC-006 and by RFBR grant № 01-02-17493.

References

1.*Pine D.J., Weitz D.A., Chaikin P.M., and Herbolzheimer E.* Diffusing-light spectroscopy. Phys. Rev. Lett. 60, 1134-1137 (1988).

2. *Maret G. and Maret G.* Multiple light scattering from disordered media. The effect of Brownian motion of scatterers. Z. Phys. B 65, 409-413 (1987).

3. *Menon N and Durian D.J.* Diffusing-wave spectroscopy of dynamic in a three-dimensional granular flow. Science 275, 1920-1922 (1997).

4. *Kao M.H., Yodh A.G., and Pine D.J.* Observation of Brownian motion on the time scale of hydrodynamic interactions. Phys. Rev. Lett. 70, 242-245 (1993).

5. *Yodh A.G., Georgiades N., and Pine D.J.* Diffusing-wave interferometry. Optics Communications 83, 56-59 (1991).

6. *Boas D.A., Bizheva K.K., and Siegel A.M.* Using dynamic low-coherence interferometry to image Brownian motion within highly scattering media. Optics Letters 23, 1087-1089 (1998).

7. *Stern M.D.* In vivo evaluation of microcirculation by coherent light scattering. Nature (London) 254, 56-58 (1975).

8. *Essex T.J.H. and Byrne P.O.* A laser Doppler scanner for imaging blood flow in skin. J. Biomed. Eng. 13, 189-194 (1991).

9. *Boas D.A. and Yodh A.G.* Spatially varying dynamical properties of turbid media probed with diffusing temporal light correlation. J. Opt. Soc. Am. A 14, 192-215 (1997).

10. *Fercher A.F. and Briers J.D.* Flow visualization by means of single-exposure speckle photography. Optics Communications 37, 326-330 (1981).

11. *Briers J.D. and Webster S.* Laser speckle contrast analysis (LASCA): a non-scanning, full-field technique for monitoring capillary blood flow. J. Biomed. Opt. 1, 174-179 (1996).

12. *Sadhwani A., Schomacker K.T., Tearney G.J., and Nishioka N.S.* Determination of Teflon thickness with laser speckle. I. Potential for burn depth diagnostics. Appl. Opt. 35, 5727-5735 (1996).

13. *Jacques S.L. and Kirkpatrick S.J.* Acoustically modulated speckle imaging of biological tissues. Opt. Lett. 23, 879-881 (1998).

14. *Dunn A.K., Bolay H., Moskowitz M.A. and Boas D.A.* Dynamic imaging of cerebral blood flow using laser speckle. Journal of Cerebral Blood Flow and Metabolizm 21, 195-201 (2001).

15. *M.P. van Albada and Lagendijk A.* Observation of weak localization of light in arandom medium. Phys. Rev. Lett. 55, 2692-2695 (1985).

16. *Wolf P. and Maret G.* Weak localization and coherent backscattering of photons in disordered media. Phys. Rev. Lett. 55, 2696-2699 (1985).

17. *Akkermans E., Wolf P.E., Maynard R., and Maret G.* Theoretical study of the coherent backscattering of light by disordered media. J. Phys. France 49, 77-98 (1998).

18. *Stephen M.J.* Temporal fluctuations in wave propagation in random media. Phys. Rev. B 37, 1-5 (1988).

19. *MacKintosh F.C. and John S.* Diffusing-wave spectroscopy and multiple scattering of light in correlated random media. Phys. Rev. B 40, 2382-2406 (1989).

20. *John S. and Stephen M.* Wave propagation and localization in a long-range correlated random potential. Phys. Rev. B 28, 6358-6369 (1983).

21. *Ackerson B.J., Dougherty R.L., Reguigui N.M. and Nobbman U.* Correlation transfer: application of radiative transfer solution methods to photon correlation problems. J. Thermophys. And Heat Trans. 6, 577-588 (1992).

22. *MacKintosh F.C., Zhu J.X., Pine D.J. and Weitz D.A.* Polarization memory of multiply scattered light. Phys. Rev. B 40, 9342-9345 (1989).

23. *Bicout D., Brosseau C., Martinez A.S. and Schmitt J.M.* Depolarization of multiply scattering waves by spherical diffusers: influence of size parameter. Phys. Rev. E 49, 1767-1770 (1994).

24. *Zimnyakov D.A. and Tuchin V.V.* About interrelations of distinctive scales of depolarization and decorrelation of optical fields in multiple scattering. JETP Letters 67, 455-460 (1998).

25. *Zimnyakov D.A.* On some manifestations of similarity in multiple scattering of coherent light. Waves in Random Media 10, 417-434 (2000).

26. *Zimnyakov D.A., Zakharov P.V., Trifonov V.A. and Chanilov O.I.* Study of interface evolution in porous media with the use of dynamic light scattering. JETP Letters 74, 237-243 (2001).

27. *Lemieux P.-A., Vera M.U. and Durian D.J.* Diffusing-light spectroscopies beyond the diffusion limit: The role of ballistic transport and anisotropic scattering. Phys. Rev. E 57, 4498-4515 (1998).

28. *Shaw T.M.* Drying as an immiscible displacement process with fluid counterflow. Phys. Rev. Lett. 59, 1671-1674 (1987).

29. *Pietronero L., Tosatti E.* Eds. Fractals in Physics, North-Holland, Amsterdam (1986).

30. *Feder J.* Fractals, Plenum Press, New York (1988).

31. *Sobol E., Sviridov A.,Omel'chenko A., Bagratashvili V, Kitai M., Harding E., Jones N., Jumel K., Mertig M., Pompe W., Ovchinnikov Y., Shekhter A. and Svistuchkin V.* Laser reshaping of cartilage. Biotech Genetic Eng Rev. 17, 553-577 (2000).

32. *Wong J.F., Milner T.E., Kim H.H., Nelson J.S. and Sobol E.N.* Stress relaxation of porcine septal cartilage during Nd:YAG (1.32(m) laser irradiation: mechanical, optical, and thermal responses. Journal of Biomedical Optics 3, 409-414, (1998).

33. *Sobol E., Sviridov A., Omel'chenko A., Bagratashvili V., Bagratashvili N. and Popov V.* Mechanism of laser-induced stress relaxation in cartilage. Proc. SPIE 2975, 310-315 (1997).

34. *Wall M.S., Deng X.-H., Torzilli P.A., Doly S.B., O'Brien S.J. and Warren R.F.* Thermal modification of collagen. J. Shoulder Elbow Surg., 8, 339-344 (1999).

35. *Bagratashvili V., Bagratashvili N., Sviridov A., Sobol E., Omel'chenko A., Tsypina S., Gapontsev V., Samartsev I., Feldchtein F. and Kurano R.* Kinetics of water transfer and stress relaxation in cartilage heated with 1.56 μm fiber laser. Proc.SPIE 3914, 102-107 (2000).

36. *Hale G.M. and Querry M.R.* Optical constants of water in the 200 nm to 200 μm wavelength region. Applied Optics 12, 555-563 (1973).

37. *Wong B.J., Milner T.E., Harrington A., Ro J., Dao X., Sobol E.N. and Nelson J.S.* Feedback-controlled laser-mediated cartilage reshaping. Arch. Facial Plast. Surg., 1, 282-287 (1999).

38. *Maitland D.J. and Walsh J.T.* Quantitative measurements of linear

birefringence during heating of native collagen. Lasers in Surgery and Medicine, 20, 310-318 (1997).

39. *Sobol E.N., Bagratashvili V.N., Sviridov A.P., Omel'chenko A.I., Ovchinnikov Yu.M., Shekhter A.B. and Helidonis E* . Cartilage shaping under laser radiation. Proc. SPIE, 2128, 43-47 (1994).

40. *Sviridov A.P., Sobol E.N., Jones N. and Lowe J.* Effect of Holmium laser radiation on stress, temperature and structure in cartilage. Lasers in Medical Science, 13, 73-77 (1998).

41. *Jamieson A.M., Blackwell J., Reihanian H., Ohno H., Gupta R., Carrino D.A., Caplan A.I., Tang L.H. and Rosenberg L.C.* Thermal and solvent stability of proteoglycan aggregates by quasielastic laser light-scattering. Carbohydrate Research, 160, 329-341 (1987).

Saratov State University
Institute of Laser and Information Technologies of Russian Academy of Sciences, Almus Ltd

Received 25.06.2002

УДК 535.361

СПЕКЛ-ДИАГНОСТИКА РЕЛАКСАЦИОННЫХ ПРОЦЕССОВ В НЕСТАЦИОНАРНЫХ РАССЕИВАЮЩИХ СИСТЕМАХ

Д.А. Зимняков, А.П. Свиридов, А.И. Омельченко, В.А. Трифонов, Д.Н. Агафонов, П.В. Захаров, Л.В. Кузнецова

Рассмотрен когерентно-оптический метод исследования процессов нестационарного массопереноса в рассеивающих средах на основе статистического анализа пространственно-временных флуктуаций интенсивности спекл-модулированных оптических полей, рассеянных объектами. В качестве примеров рассмотрены: анализ нестационарного массопереноса при испарении насыщающей жидкости из неупорядоченного пористого слоя и анализ структурной модификации хрящевой ткани в процессе ее нагрева ИК лазерным излучением. В случае испарения жидкости из пористого слоя обнаружен эффект аномального уширения спектра флуктуаций интенсивности спекл-модулированного рассеянного излучения при уменьшении скорости испарения жидкой фазы, обусловленный особенностями развития фрактального фронта испарения. Характерной особенностью термической модификации структуры хрящевой ткани является существование гистерезиса зависимости контраста спеклов, модулирующих изображение исследуемой ткани в когерентном свете, от температуры ткани в зоне модификации. Механизм структурной модификации хрящевой ткани предположительно связан с термически активированным переходом «связанная вода - свободная вода» в структуре протеогликановых агрегатов как одной из базовых составляющих хрящевой ткани.

Dmitry A. Zimnyakov was born in 1956 in Saratov. He received his degree of Doctor of Science in Physics and Mathematics at from Saratov State University. He is a Professor of the Optics Department of Saratov State University. He is an author of more than 120 scientific papers, textbooks and book chapters, editor and co-editor of 4 SPIE Proceedings books. His scientific interests include the statistical optics, biomedical optics and biophysics.

Alexander P. Sviridov was born in 1952 in Zhitomir (Ukraine). He is PhD, Senior Scientist of Institute of Information and Laser Technologies of Russian Academy of Sciences. Author of about 90 articles in the fields of laser interaction with materials, spectroscopy. He specialized mostly in the studies of optical properties, non-invasive diagnostics of biological tissues and development of hyperthermal laser technologies for medical applications.

Alexander I. Omel'chenko was born in 1954 in Berdsk, Novosibirsk reg. He received his degree of Candidate of Science in Phys. and Math. at the Institute of Nuclear Physics in Tashkent. He is a Senior Research Scientist of the Biophotonics laboratory at the Institute of Laser and Information Technologies. He is an author of more than 60 scientific papers and contributions in scientific journals. His research interests are connected with biomedical optics and biomechanics.

Valery V. Trifonov was born in 1952 in Saratov. He is a Vice-Director of Precision Mechanics and Control Institute of Russian Academy of Sciences and a President of «Almus» Company. He is a co-author of 10 scientific papers. His scientific interests include the laser metrology and optical methods of material testing.

Dmitry N. Agafonov was born in 1976 in Saratov. He graduated from Saratov State University in 1999. He is a PhD student of the Optics Department of Saratov State University. He is a co-author of 11 scientific papers. His scientific interests include the statistical optics and biomedical optics. He is a SPIE student member.

Pavel Zakharov graduated from Saratov State University in 2000 with specialty of Biomedical Optics and Laser Biophysics. Now he is a PhD student in the Optics Department and his research is focused on speckle correlometry of non-stationary mass transfer in porous media. His scientific interests cover the fields of coherent optics, novel techniques of digital signal processing, data acquisition systems. He is a SPIE student member.

Liana V. Kuznetsova was born in 1979 in Tbilisi. She graduated from Saratov State University in 2002. She is a PhD student of the Optics Department of Saratov State University. She is a co-author of 8 scientific papers. Her scientific interests are connected with biomedical optics and biophysics. She is a SPIE student member.